Global distribution of the solar wind during solar cycle 23: ACE observations

L. Zhao,[1] T. H. Zurbuchen,[1] and L. A. Fisk[1]

Received 15 May 2009; revised 17 June 2009; accepted 25 June 2009; published 28 July 2009.

[1] The composition of the solar wind can be used to determine its origin at the Sun; e.g., solar wind from coronal holes has demonstrably lower charge states than solar wind of other origins. The O^{7+}/O^{6+} ratio as measured by *Advanced Composition Explorer (ACE)* during 1998–2008 is used to divide the solar wind into three categories: non-transient solar wind from coronal holes (hereafter referred to as CHW); non-transient solar wind that originates from outside of coronal holes (hereafter referred to as NCHW), and solar wind associated with transient interplanetary coronal mass ejections (ICMEs). The global distribution of the solar wind relative to the Heliospheric Current Sheet (HCS), as specified by a Potential-Field-Source-Surface model, is then determined. The solar wind from outside of coronal holes is found to originate from a band of about 40° in width about the HCS during solar maximum conditions, and a much smaller band of < 17° during solar minimum. These results are consistent with models for the global transport of the solar magnetic field during the solar cycle, and they are consistent with earlier global flow structure determinations based upon velocity alone. **Citation:** Zhao, L., T. H. Zurbuchen, and L. A. Fisk (2009), Global distribution of the solar wind during solar cycle 23: ACE observations, *Geophys. Res. Lett.*, *36*, L14104, doi:10.1029/2009GL039181.

1. Introduction

[2] There has been general agreement for decades that fast solar wind originates from coronal holes [*Zirker*, 1977; *McComas et al.*, 1998a], and slow solar wind is related to the streamer belt regions [*McComas et al.*, 1998b; *Hundhausen*, 1977; *Gosling et al.*, 1981]. However, problems arise when using this speed separation to differentiate the solar wind origins. The solar wind speed is affected by dynamic interactions in the heliosphere, to the extent that low-speed wind (V < 600 km s^{-1}) can also appear to originate in coronal holes observed at 1 AU [*McComas et al.*, 2002]. Unlike the speed, solar wind composition signatures are independent of dynamic effects in the heliosphere and are more directly related to the solar wind coronal origins, therefore they can be used to distinguish among solar wind samples of different origins. The ionic charge composition of the solar wind is expected to become frozen-in at several solar radii, and reflects the electron temperature in the corona [*Hundhausen*, 1972]. Solar wind samples with different ionic charge composition thus must have different origins in the corona.

[3] CHW is a particularly good example where the observed composition directly mirrors the expected conditions in the corona. Coronal holes, which are regions of pronounced magnetic divergence in the corona, are observed to have low coronal electron temperatures [*Dwivedi et al.*, 2000], and similarly, the ionic charge states of the solar wind, e.g., the O^{7+}/O^{6+} ratio, indicate a freezing-in temperature of coronal electrons of only $\sim$1*MK* [*von Steiger et al.*, 1997].

[4] There are also samples of the non-transient solar wind that have higher O^{7+}/O^{6+} ratios, and thus higher freeze-in temperatures [*von Steiger et al.*, 2000]. We expect an origin for these samples of solar wind to be outside of coronal holes, and we will refer to these samples of the solar wind as NCHW. In fact, large coronal loops, on the quiet-Sun outside of coronal holes, have composition very similar to the NCHW. The coronal loops can have temperatures $\sim$1.7*MK*, comparable to the freeze-in temperatures inferred from the solar wind charge states [*Feldman et al.*, 2005]. These observations have led to theories in which these other samples of the solar wind are the result of the release of material from coronal loops. The loop temperature determines the coronal electron temperature of the released material and thus the elevated solar wind charge states [*Fisk et al.*, 1998; *Fisk*, 2003].

[5] In this paper we are concerned with the global distribution on the Sun of the two different samples of the non-transient solar wind throughout the solar cycle. We use the solar wind ionic charge composition data from the *SWICS* instrument on the *Advanced Composition Explorer (ACE)* to identify CHW and NCHW during 1998–2008. We then determine the distribution of NCHW, relative to the heliospheric current sheet (HCS) as specified by a Potential-Field-Source-Surface (PFSS) model [*Hoeksema et al.*, 1982]. We find that NCHW originates from a band of about 40° in width about the HCS at solar maximum, and a much smaller band of <17° at solar minimum.

[6] We are not specifically concerned with disturbances associated with Interplanetary Coronal Mass Ejections (ICMEs), and we thus begin by developing a compositional criterion for identifying ICMEs, and removing them from the analysis of the global distribution of the non-transient solar wind. We then establish a criterion based on the observed O^{7+}/O^{6+} ratio that allows us to distinguish between CHW and NCHW in the ordinary solar wind. We use a PFSS model to determine the location of the HCS, and use only those time periods when the predicted location of the HCS is consistent with the HCS crossings observed by ACE. We then calculate the global distribution of solar wind relative to the HCS. In Concluding Remarks we discuss

[1]Department of Atmospheric, Oceanic and Space Sciences, University of Michigan, Ann Arbor, Michigan, USA.

0094-8276/09/2009GL039181

Table 1. In Situ Signatures of ICMEs and the Expected Values in the Ambient Solar Wind[a]

	Signature	V_{sw} Relationship
1	O^{7+}/O^{6+}	$O^{7+}/O^{6+} \geq 6.008e^{(-0.00578V_{sw})}$
2	$\langle Q\rangle F_e$	$\langle Q\rangle F_e \geq 12.2 - 0.000857v_{sw}$
3	H_e/H	$H_e/H \geq 0.06$

[a][*Richardson and Cane*, 2004].

how our result is consistent with models for the global transport of magnetic field on the Sun developed by Fisk & colleagues [*Fisk et al.*, 1999; *Fisk and Schwadron*, 2001; *Fisk*, 2005].

2. Analysis

2.1. Identifying ICMEs

[7] A detailed list of ICMEs in the near-Earth solar wind during 1996–2002, given by *Cane and Richardson* [2003] (hereinafter referred to as CR03) identifies ICMEs primarily based on solar wind plasma and magnetic field signatures without reference to compositional data. Based on CR03, *Richardson and Cane* [2004] developed a subset of criteria for identifying ICME, as labeled (1), (2), and (3) in Table 1.

[8] We first test all combinations of the criteria listed in Table 1 to identify ICMEs during the 1998–2002 time period covered by CR03. We find that the ICME list identified only by criterion (1) gives the highest overlap percentage with CR03 (83.2%) and lowest 'false hit' percentage (18.3%). We judge the overlap of over 80% to be sufficient, and use the criterion (1) to identify ICMEs in our data set.

2.2. Distinguishing CHW From NCHW

[9] CHW is distinguishable by relatively low charge states in the solar wind, corresponding to low coronal electron temperatures. We set the criterion for CHW to be $O^{7+}/O^{6+} < 0.145$; with NCHW to have $O^{7+}/O^{6+} > 0.145$. The percentages of the two different types of solar wind are relatively insensitive to small deviations about the ratio of 0.145, and thus this ratio provides a reasonable demarcation between those two types of solar wind. Note that this threshold is slightly larger than the one ($O^{7+}/O^{6+} = 0.1$) as suggested by *Zurbuchen et al.* [2002], which is derived from *ULYSSES/SWICS* data at solar minimum condition.

[10] We therefore have criteria for distinguishing among ICMEs, CHW, and NCHW (Table 2). Figure 1 provides an overview of the solar wind distribution in the *ACE/SWICS* data set from 1998 to 2008, or essentially over a solar cycle. It is evident in Figure 1 that NCHW fills a large portion of the time during this solar cycle near the solar equatorial plane, where *ACE* is located: on the average, 42% of all the solar wind in the ecliptic plane at 1 AU originates from outside of coronal holes. Note that the accuracy of the ICMEs fraction in Figure 1 is about 80% as discussed in section 2.1.

2.3. Mapping the Observations Back to 2.5 Solar Radii

[11] We next map the observed solar wind data back to 2.5 solar radii, the traditional source-surface location in PFSS models. We assume as did *Neugebauer et al.* [2002] that solar wind plasma propagates radially from the source surface to the spacecraft at a constant speed, which we take to be the observed proton speed. The longitude of the solar wind source region on the surface should equal the mapped heliographic longitude added to the number of degrees that the Sun rotates during the propagation time to 1 AU. Note that the heliographic longitude and the time of the observation have a simple linear relation in each Carrington rotation: the beginning time of the Carrington rotation corresponds to heliographic longitude 360° on the source surface and the end time of the Carrington rotation corresponds to heliographic longitude 0°.

2.4. Identifying the Heliospheric Current Sheet

[12] We next use a PFSS model to determine the location of the Heliospheric Current Sheet at 2.5 solar radii for each Carrington rotation. We are interested only in those Carrington rotations when the PFSS model accurately predicts the HCS crossings at *ACE*, which we identify by using magnetic field observations from *ACE* [*Smith et al.*, 1998]. We examine the deviations of the observed magnetic field from the Parker spiral [*Parker*, 1958]. The HCS separates unipolar regions that we define as having a persistent orientation, inward or outward, lasting more than 4 days. A 4-day interval is an appropriate criterion since a <2-day interval introduces spurious field reversals, and a longer interval introduces an unacceptably large uncertainty in the location of the HCS. The crossings derived by our method were tested and found to be quite consistent with results given by *Riley et al.* [2002].

2.5. Distribution of the Solar Wind on the Source Surface

[13] Figure 2 illustrates our mapping technique for Carrington rotation 1964. PFSS results are taken from the magnetogram observations posted on the Wilcox Solar Observatory website (http://wso.stanford.edu). Note that this is an example where the location of the HCS predicted by the PFSS model is reasonably consistent with the *ACE* observations. We repeat this analysis for all Carrington rotations for which the HCS predicted by the PFSS model is consistent with the observed HCS crossings. We require that (1) the predicted PFSS HCS should intersect the spacecraft's path as many times as observed; (2) the maximum normal distances from the crossings of the observed HCS to the PFSS HCS contour (hereafter uncertainty distances) should be less than 30°. There are 29 Carrington rotations in which these two requirements are fulfilled.

Table 2. In Situ Signatures of Three Types of Solar Wind

	Signature	V_{sw} Relationship	Averaged Speed (kms^{-1})	Criterion For
1	O^{7+}/O^{6+}	$O^{7+}/O^{6+} \geq 6.008e^{(-0.00578V_{sw})}$	525	ICMEs
2	O^{7+}/O^{6+}	$0.145 < O^{7+}/O^{6+} < 6.008e^{(-0.00578V_{sw})}$	310	NCHW
3	O^{7+}/O^{6+}	$O^{7+}/O^{6+} \leq 0.145$	471	CHW

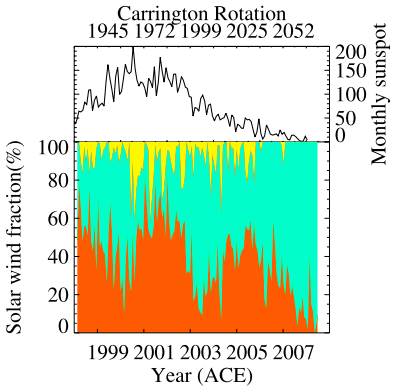

Figure 1. (top) Sunspot number and (bottom) three solar wind components during 1998–2008: ICMEs (yellow), CHW (green) and NCHW (orange).

[14] For the selected 29 Carrington rotations, we calculate the normal distance from every source point of the solar wind to the PFSS HCS contour. As shown in Figure 3, the distributions of the normal distances for CHW and for NCHW are quite different. In case of wind from outside of coronal holes, the distribution of the normal distance has a peak around 4°, and the majority of the distances distribute around this peak within about 20°, which can be considered the half-width of NCHW band. CHW, however, has a distribution of the normal distance with a peak around 35°, and the majority of the normal distances distribute from 20° to 50° around this peak.

[15] We also evaluate the distributions of normal distances for both solar maximum and solar minimum conditions. In the 29 Carrington rotations used in Figure 3, there are nine (lie in 2000–2002) during solar maximum and seven (lie in 2004–2007) during solar minimum. Repeating the statistical process discussed above, we find that in solar maximum the averaged width of the band around the HCS of NCHW solar wind is about 46°, and in solar minimum conditions the averaged width is narrowed to 17°.

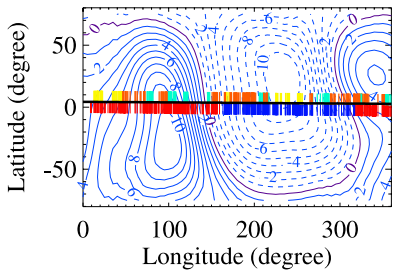

Figure 2. Origin of three types of solar wind on 2.5 solar radii surface in Carrington rotation 1964. The dashed and solid contour lines represent the inward (toward the Sun) and outward magnetic field, respectively. The purple contour line is the profile of the HCS. The color band shows the mapping results from *ACE*, in which the black line in the middle is the trajectory of the spacecraft, the color bars above the black line indicate the three types of solar wind (color convention is the same as in Figure 1) and the color bars under the black line show the magnetic polarities (inward in blue and outward in red).

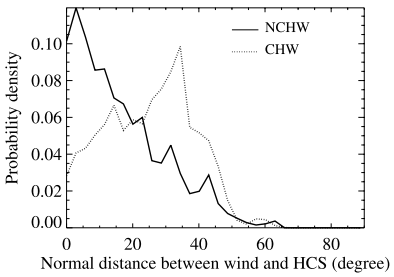

Figure 3. Probability density of the normal distance from the source of NCHW (solid line) and CHW (dotted line) to the local HCS on 2.5 solar radii surface.

[16] There is an uncertainty in our normal distance measurements that we estimate to be about 10°. We note, however, that when the deviation between PFSS model and observed HCS decreases, the normal distance from NCHW to the PFSS HCS will also decrease, but it will never increase. Hence, we interpret the width of the region that gives rise to NCHW to be in the range from ~46° to ~26° at solar maximum and <17° at this solar minimum. Interestingly, we notice that this <17° width of the streamer wind source region at the current solar minimum is narrower than last minimum, resulting in a possible 22-year cycle: the width of the streamer belt was ~40° in 1996, ~16° in 1986, and >28° in 1976 [*Richardson and Paularena*, 1997]. We thus estimate that wind from outside of coronal holes occupies about 15% of the whole solar surface at solar minimum, and can be come from as much as 80% of the solar surface at solar maximum. Note that these estimations are solely based on observations in the ecliptic plane, and a combination with the high latitude measurements (i.e., *ULYSSES*) can help to provide a more complete picture of the global solar wind.

3. Concluding Remarks

[17] We have analyzed *ACE* data for solar cycle 23 and concluded that solar wind that does not appear to be associated with coronal holes originates from a band that surrounds the HCS, and that this band has a varying width over the solar cycle, very narrow at solar minimum and quite wide at solar maximum. This result is consistent with the early study of *Zhao and Hundhausen* [1981], in which they related the observed solar wind properties in the ecliptic plane to their distance from the HCS. And our result is also consistent with models for the global transport of the magnetic field of the Sun that have been developed by Fisk and colleagues [*Fisk et al.*, 1999; *Fisk and Schwadron*, 2001; *Fisk*, 2005]. In these models differential rotation in the well-developed polar coronal holes at solar minimum drives open magnetic flux (the component of the solar magnetic field that opens into the heliosphere) into the closed field regions at the base of the HCS. The open flux is required to reconnect with the closed magnetic flux in order to maintain a continuous flow pattern of open flux around the Sun. The reconnection of open flux with coronal loops at the base of the HCS releases material forming this NCHW in a narrow band surrounding the HCS.

[18] At solar maximum conditions there are no well-developed polar coronal holes to drive the open flux into

a narrow band around the HCS; rather there are more transient coronal holes located at various latitudes on the Sun. In the models of Fisk & colleagues there is still transport of open flux at solar maximum driven by the motion of the open flux in the transient coronal holes, by reconnection of open flux with the active magnetic field on the Sun at solar maximum, as well as by the general rotation of the HCS. The reconnections associated with this transport of open flux at solar maximum should also release solar wind and create the broader distribution of solar wind from outside of coronal holes that is observed.

[19] The association of NCHW with the HCS could suggest that it is the dynamics of the streamer belt, the large coronal loops and helmet structures that underlie the HCS, which is the governing mechanism for the origination of NCHW. Perhaps there are instabilities in the streamer belt that release what are effectively small CMEs; indeed, Shelley & colleagues observe the outflows of density concentrations near the HCS [*Sheeley and Wang*, 2007]. However, the streamer belt is not demonstrably wider at solar maximum compared to solar minimum, which suggests that the global structure of the solar magnetic field and the absence or presence of well-defined polar coronal holes is more important in determining the global distribution of the solar wind that does not originate from coronal holes.

[20] **Acknowledgments.** This work was supported, in part, by NASA contracts NAG5-12929 and NNG04GN73G and JPL subcontract 1268016. We acknowledge the use of publicly available data products from ACE-SWEPAM, *ACE*-SWICS, *ACE*-MAG, and Wilcox. We acknowledge helpful discussions and advice from J. T. Gosling. We also acknowledge great help from S. Lepri, J. Gilbert, and D. Eddy.

References

Cane, H. V., and I. G. Richardson (2003), Interplanetary coronal mass ejections in the near-Earth solar wind during 1996–2002, *J. Geophys. Res.*, *108*(A4), 1156, doi:10.1029/2002JA009817.

Dwivedi, B. N., A. Mohan, and K. Wilhelm (2000), On the electron temperatures, densities and hot ions in coronal hole plasma observed by SUMER on SOHO, *Adv. Space Res.*, *27*, 1751.

Feldman, U., E. Landi, and N. A. Schwadron (2005), On the sources of fast and slow solar wind, *J. Geophys. Res.*, *110*, A07109, doi:10.1029/2004JA010918.

Fisk, L. A. (2003), Acceleration of the solar wind as a result of the reconnection of open magnetic flux with coronal loops, *J. Geophys. Res.*, *108*(A4), 1157, doi:10.1029/2002JA009284.

Fisk, L. A. (2005), The open magnetic flux of the Sun. I. Transport by reconnections with coronal loops, *Astrophys. J.*, *626*, 563.

Fisk, L. A., and N. A. Schwadron (2001), The behavior of the open magnetic field of the Sun, *Astrophys. J.*, *560*, 425.

Fisk, L. A., N. A. Schwadron, and T. H. Zurbuchen (1998), On the slow solar wind, *Space Sci. Rev.*, *86*, 51.

Fisk, L. A., T. H. Zurbuchen, and N. A. Schwadron (1999), On the coronal magnetic field: Consequences of large-scale motions, *Astrophys. J.*, *521*, 868.

Gosling, J. T., G. Borrini, J. R. Asbridge, S. J. Bame, W. C. Feldman, and R. T. Hansen (1981), Coronal streamers in the solar wind at 1 AU, *J. Geophys. Res.*, *86*, 5438.

Hoeksema, J. T., J. M. Wilcox, and P. H. Scherrer (1982), Structure of the heliospheric current sheet in the early portion of sunspot cycle 21, *J. Geophys. Res.*, *87*, 10,331.

Hundhausen, A. J. (1972), *Coronal Expansion and Solar Wind*, *Phys. Chem. Space*, vol. 5, Springer, New York.

Hundhausen, A. J. (1977), An interplanetary view of coronal holes, in *Coronal Holes and High Speed Streams*, edited by J. Zirker, p. 225, Colo. Assoc. Univ. Press, Boulder.

McComas, D. J., P. Riley, J. T. Gosling, A. Balogh, and R. Forsyth (1998a), Ulysses' rapid crossing of the polar coronal hole boundary, *J. Geophys. Res.*, *103*, 1955.

McComas, D. J., et al. (1998b), Ulysses' return to the slow solar wind, *Geophys. Res. Lett.*, *25*, 1.

McComas, D. J., H. A. Elliott, J. T. Gosling, D. B. Reisenfeld, R. M. Skoug, B. E. Goldstein, M. Neugebauer, and A. Balogh (2002), Ulysses' second fast-latitude scan: Complexity near solar maximum and the reformation of polar coronal holes, *Geophys. Res. Lett.*, *29*(9), 1290, doi:10.1029/2001GL014164.

Neugebauer, M., P. C. Liewer, E. J. Smith, R. M. Skoug, and T. H. Zurbuchen (2002), Sources of the solar wind at solar activity maximum, *J. Geophys. Res.*, *107*(A12), 1488, doi:10.1029/2001JA000306.

Parker, E. N. (1958), Dynamics of the interplanetary gas and magnetic fields, *Astrophys. J.*, *128*, 664.

Richardson, I. G., and H. V. Cane (2004), Identification of interplanetary coronal mass ejections at 1 AU using multiple solar wind plasma composition anomalies, *J. Geophys. Res.*, *109*, A09104, doi:10.1029/2004JA010598.

Richardson, J. D., and K. I. Paularena (1997), Streamer belt structure at solar minima, *Geophys. Res. Lett.*, *24*, 1435.

Riley, P., J. A. Linker, and Z. Mikić (2002), Modeling the heliospheric current sheet: Solar cycle variations, *J. Geophys. Res.*, *107*(A7), 1136, doi:10.1029/2001JA000299.

Sheeley, N. R., Jr., and Y. M. Wang (2007), In/out pairs and the detachment of coronal streamers, *Astrophys. J.*, *655*, 1142.

Smith, C. W., J. L'Heureux, N. F. Ness, M. H. Acuña, L. F. Burlaga, and J. Scheifele (1998), The ACE magnetic fields experiment, *Space Sci. Rev.*, *86*, 611.

von Steiger, R., J. Geiss, and G. Gloeckler (1997), *Cosmic Winds and the Heliosphere*, *Space Sci. Ser.*, edited by J. R. Jokipii, C. P. Sonett, and M. S. Giampapa, Univ. of Ariz. Press, Tucson.

von Steiger, R., N. A. Schwadron, L. A. Fisk, J. Geiss, G. Gloeckler, S. Hefti, B. Wilken, R. R. Wimmer-Schweingruber, and T. H. Zurbuchen (2000), Composition of quasi-stationary solar wind flows from Ulysses/Solar Wind Ion Composition Spectrometer, *J. Geophys. Res.*, *105*, 27,217.

Zirker, J. B. (1977), Coronal holes and high-speed wind streams, *Rev. Geophys.*, *15*, 257.

Zhao, X.-P., and A. J. Hundhausen (1981), Organization of solar wind plasma properties in a tilted, heliomagnetic coordinate system, *J. Geophys. Res.*, *86*, 5423.

Zurbuchen, T. H., L. A. Fisk, G. Gloeckler, and R. von Steiger (2002), The solar wind composition throughout the solar cycle: A continuum of dynamic states, *Geophys. Res. Lett.*, *29*(9), 1352, doi:10.1029/2001GL013946.

L. A. Fisk, L. Zhao, and T. H. Zurbuchen, Department of Atmospheric, Oceanic and Space Sciences, University of Michigan, 2455 Hayward Street, Ann Arbor, MI 48109-2143, USA. (lzh@umich.edu)